Phytoplankton growth and consumption by microzooplankton stimulated by turbulent nitrate flux suggest rapid trophic transfer in the oligotrophic Kuroshio

Toru Kobari[1*], Taiga Honma[2], Daisuke Hasegawa[3], Naoki Yoshie[4], Eisuke Tsutsumi[5], Takeshi Matsuno[6], Takeyoshi Nagai[7], Takeru Kanayama[2], Fukutaro Karu[2], Koji Suzuki[8], Takahiro Tanaka[3], Xinyu Guo[4], Gen Kume[1], Ayako Nishina[1] and Hirohiko Nakamura[1]

[1]Aquatic Sciences, Faculty of Fisheries, Kagoshima University
4-50-20 Shimoarata, Kagoshima, Kagoshima 890-0056, Japan
[2]Aquatic Sciences, Graduate School of Fisheries, Kagoshima University
4-50-20 Shimoarata, Kagoshima, Kagoshima 890-0056, Japan
[3]Tohoku National Fisheries Research Institute, Japan Fisheries Research and Education Agency
3-27-5 Shinhama-cho, Shiogama, Miyagi 985-0001, Japan
[4]Center for Marine Environmental Studies, Ehime University
2-5 Bunkyo-cho, Matsuyama, Ehime 790-8577, Japan
[5]Atmosphere and Ocean Research Institute, University of Tokyo
5-1-5 Kashiwanoha, Kashiwa, Chiba 277-8564, Japan
[6]Research Institute for Applied Mechanics, Kyushu University
6-1 Kasuga-koen, Kasuga, Fukuoka 816-8580, Japan
[7]Department of Ocean Sciences, Tokyo University of Marine Science and Technology
4-5-7 Konan Minato-ku, Tokyo 108-8477, Japan
[8]Faculty of Environmental Earth Science, Hokkaido University
North 10 West 5 Kita-ku, Sapporo, Hokkaido 060-0810, Japan

Correspondence to: Toru Kobari (kobari@fish.kagoshima-u.ac.jp)

Abstracts. The Kuroshio Current has been thought to be biologically unproductive due to oligotrophic conditions and low plankton standing stocks. Even though vulnerable life stages of major foraging fishes have a risk to be entrapped by frontal eddies and meanders and encountered under the low food availability, they have life cycle strategies to grow and recruit around the Kuroshio Current. Here we report that phytoplankton growth and consumption by microzooplankton is stimulated by turbulent nitrate flux amplified with the Kuroshio Current. Oceanographic observations demonstrate that the Kuroshio Current topographically enhances significant turbulent mixing and nitrate influx to the euphotic zone. Gradual nutrient enrichment experiments show growth rates of phytoplankton and micro-heterotrophs communities were stimulated within a range of the turbulent nitrate flux. Results of dilution experiments imply a significant microzooplankton grazing on phytoplankton. We propose that these rapid and systematic trophodynamics enhance biological productivity in the Kuroshio.

37 **1 Introduction**

38 The Kuroshio Current is the western boundary current of the North Pacific Subtropical Gyre (Qiu, 2001; Hu et
39 al., 2015). The Kuroshio enters the East China Sea from the east of Taiwan and flows along the continental slope until it
40 passes through the Tokara Strait into the western North Pacific (Fig 1a). The Kuroshio has been thought to be biologically
41 unproductive because ambient nutrient concentrations and plankton standing stocks in its waters are low (Guo, 1991;
42 Hirota, 1995). In spite of such seemingly unproductive conditions, the Kuroshio in the East China Sea (ECS-Kuroshio)
43 is neighboring major spawning and nursery grounds for foraging species such as sardine (Watanabe et al., 1996), jack
44 mackerel (Sassa et al., 2008), and chub mackerel (Sassa and Tsukamoto, 2010), and common squid (Bower et al., 1999).
45 Indeed, good fishing grounds have been formed for various fishes and squid using the Kuroshio and their catches
46 composed more than half of total catch in Japan (Saito, 2019). Highly vulnerable early life stages of many foraging species
47 have a risk to grow and recruit under the oligotrophic and unproductive waters in the ECS-Kuroshio (hereafter called the
48 “Kuroshio Paradox”: Saito, 2019), even if the warm temperatures of the Kuroshio Current could enhance cellular
49 metabolic processes and then growth. It has been believed that survival of these early stages is supported by high plankton
50 productivity on the continental shelf and in the Kuroshio front (Nakata et al., 1995). However, such good food availability
51 is spatially limited and greatly variable because the Kuroshio Current often meanders (Nakata and Hidaka, 2003).
52 Otherwise, the coastal water mass is sometimes entrapped and transported into the Kuroshio and more pelagic sites
53 (Nakamura et al., 2006; Kobari et al., 2019). Use of waters in the vicinity of the oligotrophic Kuroshio as a nursery and
54 feeding ground would therefore appear to be a risky strategy unless there is a mechanism that enhance biological
55 production in the Kuroshio.

56 There is increasing information on community structure of phyto- and zooplankton in the Kuroshio. Pico- to

57 nano-autotrophs contributed to phytoplankton standing stocks in the Kuroshio and predominant components were cellular
58 cyanobacteria like *Prochlorococcus* and *Synechococcus*, haptophytes and diatoms (Hasegawa et al., 2019; Endo and
59 Suzuki, 2019). Heterotrophic bacteria and calanoid copepods contributed to heterotrophs biomass in the Kuroshio, while
60 microzooplankton biomass were minor (Kobari et al., 2019). Based on the mass balance model, mesozooplankton
61 standing stocks were supported by micro- and nano-autotrophs and microzooplankton (Kobari et al., 2019). However, we
62 have little knowledge how biogeochemical processes and trophodynamics support plankton community in the Kuroshio.
63 In recent years, some mechanisms have been found for nutrients supply to the oligotrophic Kuroshio waters. The
64 Kuroshio nutrient stream contributed significantly to productivity in the euphotic layer, similarly to the "nutrient stream"
65 along the Gulf Stream (Komatsu and Hiroe, 2019). Turbulence around the Kuroshio appeared to be important for upward
66 nutrients supply in the Kuroshio (Nagai et al., 2019). Frontal disturbances also contributed to nutrients supply to the
67 surface layer in the Kuroshio (Kuroda, 2019). Moreover, the Island Mass Effect was produced by the Kuroshio Current
68 around the archipelagic topography and induced upward nutrients supply (Hasegawa, 2019). These nutrients supplies
69 have been suggested to stimulate biological productivity in the Kuroshio. In the wide Kuroshio track area, these nutrients
70 supplies can happen particularly around the Tokara Straits due to the extensive frontal disturbances (Nakamura et al.,
71 2006) and strong turbulence (Tsutsumi et al., 2017; Nagai et al., 2017, 2019).
72 Here we report phytoplankton productivity and subsequent microzooplankton grazing stimulated by turbulent
73 nitrate flux that can happen in the Kuroshio Current. Oceanographic observations demonstrate a significant nitrate flux
74 caused by turbulent mixing in the Tokara Strait of the ECS-Kuroshio. Nutrient-amended bottle incubation experiments
75 show phytoplankton and micro-heterotrophs growths elevated within a range of this turbulent nitrate flux and significant
76 grazing of microzooplankton on phytoplankton.

2 Materials and methods

2.1 Onboard observations and experiments

All oceanographic observations and bottle incubations were done in the Kuroshio Current where it passes through the Tokara Strait. Samplings for nitrate concentrations and measurements of turbulent diffusivity were conducted at 14 stations along the 2 lines across the Kuroshio Current (Fig 1a) during cruises of the T/S *Kagoshima-maru* in November 2015.

The nitrate profiles were measured by a nitrate sensor (Deep SUNA V2) attached on a SBE-9plus CTD system. The turbulence diffusivity was estimated from microstructure measurements by TurboMAP-L (JFE Advantech Co. Ltd.) based on Osborn (1980)'s formula, which were deployed instantly after each CTD cast for the same stations. The nitrate sensor was calibrated with the observed nitrate concentrations (Supplement Fig. 1). Since the precision of the nitrate sensor: P in this study is 0.37 mmol m^{-3} (estimated by Hasegawa et. al., 2019), if we calculate the vertical gradient from the raw data, the noise level would be too high for resolving the normal background nitrate stratification of O (10^{-1} mmol m^{-4}). Therefore, we need to apply the vertical averaging on the sensor data for reducing the sensing error. Using the sensor value: Cs, real concentration: Cr, vertical deployment speed of sensor: w, sampling frequency: f, and averaging bin size: Δz, the bin averaged vertical gradient of sensor value can be written as

$$\frac{\partial \overline{Cs}}{\partial z} \sim \frac{\overline{Cr}_i - \overline{Cr}_{i-1}}{\Delta z} \pm P\sqrt{\frac{2\overline{w}}{\Delta z^3 f}} \quad (1)$$

where, f = 1 Hz, $\overline{w}$ = 0.5 m s^{-1} in this study. The second term of the right side of Eq. (1) indicates the expected precision of the bin averaged vertical gradient of nitrate (see the detailed discussions in Hasegawa et. al., 2019). In this study, we took Δz = 10 m to resolve the realistic vertical gradient with the expected error size in O (10^{-2} mmol m^{-4}). Total of sixteen nitrate and the turbulence diffusivity profiles obtained among the stations at KG1515 cruise by T/S Kagoshima-

98 maru across the Kuroshio path were averaged, then the profiles of the gradient of the averaged nitrate, and the averaged
99 turbulence diffusivity were multiplied for each depth to get the averaged turbulent nitrate fluxes. Both parameters were
100 binned and averaged within 10-meter intervals. The vertical gradient of the averaged nitrate profile (C_{NO3}) and the
101 averaged vertical diffusivity profile (K_z) were then multiplied at each depth (z) to estimate the area-averaged vertical
102 turbulent nitrate flux (F_{NO3}) with the following equation:

103 $$F_{NO3} = -K_Z \times \partial C_{NO3} / \partial \mathrm{z} \quad (2)$$

104 In recent years, there is an active discussion about the importance of diapycnal advective flux associated with the diffusive
105 flux (e.g., Du et al., 2017); however, in the present study, we assumed that the important nutrient flux was the one across
106 the euphotic depth, not through the density layer, which was transformed by the turbulent mixing. In addition, as our
107 studied regions were frontal regions unlike the South China Sea, where the Kuroshio flows over the seamounts, density
108 fluctuations should be caused not only by turbulent mixing but also by advection and the movement of the fronts.
109 Accordingly, we focus our discussions on the vertical turbulent nutrient flux using cartesian coordinate, rather than
110 diapycnal flux using isopycnal coordinate.

111 Two different types of bottle incubations were performed in the present study. For phytoplankton and micro-
112 heterotrophs growth rates in response to *in situ* nitrate influx by turbulent mixing, bottle incubations with nutrient
113 gradients (EXP_a) were conducted at 8 stations in November 2016 and 2017. For microzooplankton grazing on
114 phytoplankton, the dilution experiments (EXP_b) followed by Landry and Hasset (1982) were done at 8 stations in
115 November 2017 (Fig 1b, Table 1).

116

117 **2.2 Experimental setup**

118 Seawater samples for all experiments were obtained using 2.5-L Niskin-X bottles attached to a conductivity-
119 temperature-depth profiler and carousel multisampling system (CTD-CMS: Sea−Bird SBE-9plus). The samples were
120 transferred by gravity filtration using a silicon tube with a nylon filter (0.1-mm mesh opening) into the incubation bottles
121 for EXP_a and EXP_b.

122 EXP_a was performed using duplicate 2.3-L polycarbonate bottles without added nutrients and with a mixture of
123 nitrate ($NaNO_3$) and phosphate (KH_2PO_4) in an atomic N:P ratio of 15:1. The nitrate concentrations were either 0 (control),
124 0.05, 0.15, 0.5, 0.75, 1.5, or 5 μmol L^{-1}. Assuming that the turbulent nitrate supplies at the subsurface chlorophyll
125 maximum observed in the Tokara Strait (*O*: 0.788 mmol m^{-2} d^{-1}, see Results) were continued during 5.3 days when the
126 Kuroshio Current (0.33 m s^{-1}, Zhu et al., 2017) passed over the Tokara Strait (150 km) and consumed by phytoplankton
127 in a 10-m thick layer, they were equivalent to the nitrate enrichment of 0.41 μmol L^{-1}.

128 EXP_b was conducted using triplicate 1.2-L polycarbonate bottles with microzooplankton as grazers and involved
129 four dilution factors (10, 30, 60, and 100%) of the microzooplankton standing stocks in the original water samples. These
130 treatment bottles were enriched with 3 μmol L^{-1} nitrate ($NaNO_3$) and 0.2 μmol L^{-1} phosphate (KH_2PO_4) to promote
131 phytoplankton growth. For evaluating nutrient limitation on phytoplankton growth, no enrichment was conducted for
132 triplicate non-diluted bottles (100%) for EXP_b.

133 All incubation tools were soaked in 10% HCl and rinsed with surface seawater at each station before use (Landry
134 et al., 1995). All experimental bottles were incubated for 72 h for EXP_a and 24 h for EXP_b in a water bath with running
135 surface seawater for temperature control and covered by a nylon mesh screening (5-mm mesh opening screening to reduce
136 irradiance to 75% of the surface irradiance. Note that the phytoplankton growth in the incubation bottles might be

overestimated due to the weaker irradiance at subsurface than those under the incubation conditions.

2.3 Sample analysis

Chlorophyll *a* concentrations were determined at the beginning and end of the incubations for EXP_a and EXP_b. Subsamples of 500 to 1000 mL were filtered through a nylon mesh (11-μm mesh opening: Millipore NY1104700) and a glass-fiber filter (2-μm: Whatman GM/F, 0.7-μm: Whatman GF/F) for EXP_a and through a glass-fiber filter (GF/F) for EXP_b at a pressure less than 20 kPa. Photosynthetic pigments were extracted overnight in *N,N*–dimethylformamide at –20°C in the dark, and the chlorophyll *a* concentrations were determined with a fluorometer (Turner Designs 10AU or TD700). Size fractions were defined as Pico for chlorophyll smaller than 2 μm, Nano for chlorophyll between 2 and 11 μm and Micro for chlorophyll larger than 11 μm.

Micro-sized heterotrophs in the incubation bottles at the beginning of EXP_a and EXP_b were examined. Subsamples of 500 mL were collected and fixed with 3% acid Lugol's solution. We identified and counted three taxonomic groups of the micro-heterotrophs community with an inverted microscope (Leica Leitz DMRD). Some marine planktonic ciliates and flagellates are known to be mixotrophs (Gaines and Elbrächter, 1987), but we assumed naked ciliates and tintinnids to be heterotrophic in the present study. The sizes of cells or individuals were measured, biovolume was computed based on geometric shape, and the carbon content was estimated using conversion equations (Put and Stoecker, 1989; Verity and Langdon, 1984; Parsons et al., 1984).

2.4 Rate calculation

Growth rates (g: d^{-1}) in the incubation bottles of EXP_a and EXP_b were calculated from size-fractionated chlorophyll *a* concentrations (μg L^{-1}) or standing stocks (μgC L^{-1}) of micro-heterotrophs groups identified at the

158 beginning (C_o) and end (C_t) of the incubations period (t: days):

159 $$G = [\ln(C_t) - \ln(C_o)]/t \quad (3)$$

160 Apparent growth rates in the incubation bottles of EXP_b were calculated using the following model (Landry et al., 1995):

161 $$C'_t = C'_o \times \exp[(g_{max} - m) \times t] \quad (4)$$

162 where g_{max} and m are the maximum growth rate of size-fractionated phytoplankton (d^{-1}) and their mortality rate by

163 microzooplankton grazing (d^{-1}), respectively. The maximum growth rate and mortality rate were determined with a linear

164 regression of the apparent growth rate against dilution factors (X):

165 $$g = g_{max} - m\mathrm{X} \quad (5)$$

166 All parameters derived from EXP_a and EXP_b are listed in Table 2 and Table 3.

167

168 **3 Results**

169 **3.1 Oceanographic observations**

170 First, turbulent diffusivity and nitrate concentrations were measured in order to estimate the vertical turbulent

171 nitrate flux along the transects across the Kuroshio Current in the Tokara Strait, where a shallow ridge lies in the

172 Kuroshio's path. We obtained 16 pairs of vertical profiles for turbulent diffusivity and nitrate concentrations and estimated

173 the averages and 95 percent confidence intervals of the vertical profiles. The averaged chlorophyll-*a* profile (Fig 2a)

174 recorded with a light-emitting diode fluorometer on a TurboMAP-L profiler revealed a subsurface chlorophyll maximum

175 (SCM) at 60 m, which was almost coincident with a sharp increase in the nitrate concentration (i.e., the top of the

176 nitracline). Vertical diffusivity of O (10^{-4} m^2 s^{-1}, Fig 2b) was higher at 70 m compared with those in the layers between

177 80 and 130 m. Just below the SCM peak, relatively high nitrate concentrations and vertical diffusivity induced vertical

178 turbulent nitrate fluxes of O (1 mmol m^{-2} d^{-1}, Fig 2c).

179

180 **3.2 Gradient enrichment experiments (EXP_a)**

181 To evaluate how these turbulent nitrate fluxes measured in the Tokara Strait increase the standing stocks of
182 phytoplankton and micro-heterotrophs in the Kuroshio, we conducted bottle incubations of the phytoplankton and micro-
183 heterotrophs communities enriched with the different nutrient concentrations (EXP_a). The total chlorophyll *a*
184 concentrations at the beginning of the EXP_a averaged among the duplicate samples ranged from 0.15 to 0.52 μg L^{-1} (Table
185 1). The pico-fractions defined as smaller than 2 μm and nano-fractions between 2 to 11 μm accounted for more than 80%
186 of the total chlorophyll *a* (Fig 3a). All size-fractionated chlorophyll *a* declined or changed little toward the end of the
187 incubations at the nitrate enrichments below 0.15 μmol L^{-1}, but they increased at the enrichments above 0.5 μmol L^{-1}. At
188 the beginning of the incubations, micro-heterotrophs standing stocks averaged among the duplicate samples ranged from
189 0.12 to 0.79 μg C L^{-1} (Table 1). Naked ciliates accounted for 51 to 96% of the micro-sized heterotrophs biomass in terms
190 of carbon at the beginning of the incubations. Copepod nauplii were the second contributor to the micro-heterotrophs
191 biomass due to the low abundance and large individual body mass, and tintinnid ciliates were a minor component. The
192 standing stocks of all taxonomic groups in the micro-sized heterotrophs increased with the higher nitrate enrichments (Fig
193 3b), but the increasing patterns to nutrient gradient were less clear than those of the size-fractionated chlorophyll *a*
194 concentrations.

195 Based on these differences of the standing stocks between the beginning and end of the incubations, we
196 investigated the growth rates of chlorophyll and micro-heterotrophs. The growth rates of all size-fractionated chlorophyll
197 increased at the larger nitrate additions (Fig 4a). Growth rates were negative or close to zero for all size-fractions at the
198 enrichment below 0.15 μmol L^{-1}. However, the pico- and micro-sized chlorophyll revealed positive growth rates at the

199 nitrate concentrations above 0.5 μmol L^{-1}, which were nearly equivalent to the turbulent nitrate fluxes observed in the
200 Tokara Strait (see Experimental setup). Because micro-heterotrophs growth rates varied among stations, the response of
201 micro-heterotrophs growth to nutrient gradient was ambiguous (Fig 4b). Growth rates were positive for copepod nauplii
202 at all nitrate enrichments and were higher for both naked and tintinnid ciliates at the larger nitrate enrichments. Thus, the
203 standing stocks of phytoplankton and micro-heterotrophs were likely increased within the range of the turbulent nitrate
204 fluxes measured in the Tokara Strait.

205 The slope of a linear regression between growth rates of the size-fractionated chlorophyll and the logarithms of
206 the nitrate enrichments at each incubation provided a metric of the sensitivity of their growth rates to nutrient supply. As
207 shown in Supplement Fig 1, the steeper slopes were found at some stations in the upstream Kuroshio in the Tokara Strait
208 compared with those at the other stations, suggesting that apparent phytoplankton growths were variable with the nutrients
209 concentrations or predatory impacts at the beginning of the incubations. To explain whether growth rates of the size-
210 fractionated chlorophyll might be variable with initial nutrients concentrations (bottom-up control) or predator biomasses
211 (top-down control) at the beginning of the experiments, the slopes were compared to the nitrate+nitrite (Fig 5a) and
212 phosphate concentrations (Fig 5b) and micro-heterotrophs biomass (Fig 5c) in the ambient seawater without enrichment.
213 No significant correlation was found for all size-fractionated chlorophyll to the micro-sized heterotrophs biomass. On the
214 other hand, there was a negative correlation of the slopes for all size-fractions to the nitrate plus nitrite or phosphate
215 concentrations, indicating that the stimulation of their growth rates by nutrients supply was greater for all size-fractionated
216 chlorophyll under more oligotrophic conditions. Thus, the variations in phytoplankton growth rates are likely associated
217 with nutrients concentrations at the beginning of the incubations.

218

3.3 Dilution experiments (EXP_b)

To evaluate how much and which size-fractionated phytoplankton was removed by microzooplankton grazing, the dilution experiments were conducted simultaneously to the gradient enrichment experiments. The maximum growth rates represented by the intercepts in the dilution experiments were relatively high for the nano-sized chlorophyll (Fig 6a), while the difference was insignificant among the three size-fractions (ANOVA, $p>0.05$). These findings indicated that growth potential under no microzooplankton grazing was slightly high for the nano-sized chlorophyll compared with those for the pico- and micro-fractions. On the other hand, the slopes were representative of the mortality rates by microzooplankton grazing and significantly higher for the nano-sized chlorophyll than those for the pico- and micro-sized chlorophyll (ANOVA+Tukey, $p<0.05$), indicating the preference of microzooplankton grazing on the nano-sized chlorophyll. To evaluate the impact of microzooplankton grazing on phytoplankton growth, we compared the three different net growth rates, which were the observed net growth rates without enrichment (g_o) and with enrichment (g_{en}) in the non-diluted bottles, and the estimated net growth rates (g_{en}') subtracted the mortality rates (m) from the maximum growth rates (g_{max}). All size-fractionated chlorophyll demonstrated g_o lower than g_{en} (Fig 7), indicating nutrient limitation on the net growth rates. Both g_{en} an g_{en}' were comparable due to no significant difference between the two (Welch's *t*-test). These results imply that g_{en} of all size-fractionated chlorophyll balances the microzooplankton grazing mortality with the maximum growth. Particularly for the nano-fractionated chlorophyll, the net growth rates were slightly low due to the mortality rates by microzooplankton grazing exceeded the maximum growth rates.

4 Discussion

The Kuroshio Current impinges on numerous shallow ridges with small islands and seamounts in the Tokara Strait. Several studies have pointed out that those steep topographic features stir and modify the water column through

upwelling (Hasegawa et al., 2004, 2008) and turbulent mixing (Tsutsumi et al., 2017; Nagai et al., 2017). Comparing with the turbulent nitrate fluxes among the previous study sites, the fluxes observed in the Tokara Strait of the Kuroshio Current were one order higher than those reported in the Kuroshio Extension front (Kaneko et al., 2012, 2013; Nagai et al., 2017), much greater than those at other oceanic sites, and equivalent to those at coastal sites (Cyr et al., 2015). The turbulent nitrate flux in the downstream Kuroshio Current where was close to the Tokara Strait was similar magnitude to our estimates (Nagai et al., 2019). Since the Kuroshio Current steadily runs in the Tokara Strait, such nutrient supply induced by turbulence diffusivity is considered as one of mechanisms that phytoplankton productivity is enhanced even under oligotrophic Kuroshio.

In spite of the large turbulent nitrate flux (O: 1 mmol m^{-2} d^{-1}), the chlorophyll *a* concentrations in the Tokara Strait of the Kuroshio Current were as low as the values reported from the neighboring Kuroshio (Kobari et al., 2018, 2019) and oceanic sites in the North Pacific Ocean (Calbet and Landry, 2004). Based on the gradient enrichment experiments, standing stocks and their growth rates of all size-fractionated phytoplankton increased at the nitrate enrichments above 0.5 μmol L^{-1} that were equivalent to the observed turbulent nitrate flux. These results suggest that phytoplankton standing stocks and growths are stimulated by the magnitude of the observed turbulent nitrate flux. In the global comparisons, microzooplankton reveal a significant grazing impact on phytoplankton, particularly in oceanic sites (Calbet and Landry, 2004). Microzooplankton standing stocks in the Kuroshio Current at the Tokara Strait were lower than those on the continental shelf of the ECS (Chen et al., 2003) and might be removed by mesozooplankton predation (Kobari et al., 2019). These results expected low microzooplankton grazing on phytoplankton. However, the dilution experiments demonstrated that phytoplankton mortality by microzooplankton grazing was significantly high and equivalent to 41 to 122% of maximum growth rates of phytoplankton based on the ratio of the mortality rate to the

maximum growth rates for total chlorophyll *a* (Table 2). Indeed, phytoplankton net growth likely balances microzooplankton grazing mortality with phytoplankton maximum growth, particularly for nano-fractionated phytoplankton (Fig. 7). These results from the simultaneously conducted experiments suggest that phytoplankton standing stocks are stimulated by turbulent nitrate flux and then quickly removed by microzooplankton grazing, particularly for nanophytoplankton. Taking into account for the size range of prey for ciliates (Pierce and Turner, 1992) and copepod nauplii (Uye and Kasahara, 1983), microzooplankton grazing would be a major reason why phytoplankton do not attain high growth rates and standing stocks, even under the high potential growth and sensitive to nutrient enrichments. Thereby, the rapid transfer of the elevated phytoplankton production to microzooplankton might be a possible mechanism of the low chlorophyll even under the large turbulent nitrate flux in the Kuroshio Current.

The standing stocks and growth rates of all micro-sized heterotrophs were relatively higher at the larger nitrate enrichments, but the increasing patterns were less clear than those of phytoplankton. This difference was probably due to the large variations in these micro-heterotrophs standing stocks among stations (Table 1) and slower growth than phytoplankton. Indeed, such unclear pattern was remarkable for copepod nauplii representing their slower growth rate, less abundance in the bottle and large individual body mass. On the other hand, “intra-guild” predation within micro-heterotrophs community might be another explanation on the less clear pattern of their standing stocks and growth rates. Growth rates of copepod nauplii were always higher than those of naked ciliates, especially under no or less nitrate supply. The ratio of mean equivalent spherical diameter of body mass between copepod nauplii (88 μm) and naked ciliates (16 μm) was estimated to be 5:1 and much different from to the predator-prey mass ratio (i.e., 18:1, Hansen et al., 1994). Thus, such intraguild predation of copepod nauplii on naked ciliates would not happen in the bottles. More importantly to no or less clear pattern of the growth of micro-heterotrophs, the results from the simultaneously conducted experiments

imply that phytoplankton productivity is stimulated by the turbulent nitrate flux and rapidly grazed by microzooplankton but standing stocks and growths of micro-heterotrophs are not elevated during 3 days in the Kuroshio Current. Increase of micro-heterotrophs standing stocks and their trophic transfer to mesozooplankton might be found in the further downstream of the Kuroshio Current.

There is increasing information that turbulence-induced nutrient fluxes have been suggested to promote phytoplankton growth in the open ocean (Kaneko et al., 2013; Nagai et al., 2017, 2019), however, no experimental documentation is available for response of phytoplankton community to the nutrient supply or of subsequent trophic transfer in a planktonic food web. In the tropical and subtropical oceans, microzooplankton grazing has been thought to be a major source of phytoplankton mortality and has been shown to account for more than 75% of phytoplankton daily growth (Calbet and Landry, 2004). Furthermore, strong trophic linkages are well known between microbes and metazoans through microzooplankton (Calbet and Landry, 1999; Calbet et al., 2001; Calbet and Saiz, 2005; Kobari et al., 2010). Our study has provided the first experimental evidence that phytoplankton standing stocks and growths are stimulated by turbulent nutrient fluxes and rapidly grazed by microzooplankton. These results imply a possibility that biological productivity is underestimated by apparent low nutrients and low phytoplankton biomass in the Kuroshio. Because strong turbulence amplified by the Kuroshio Current, phytoplankton productivity stimulated by the nutrient flux and rapid trophic transfer to microzooplankton are likely to happen in the Tokara Strait and the downstream, we propose that unobservable biological productivity in the Kuroshio is sustained by these rapid and systematic trophodynamics. Such unobservable biological production elevated by the rapid and systematic trophodynamics may provide good food availability for the vulnerable stages of foraging fishes around the Kuroshio and thus explain a part of the Kuroshio Paradox.

Data Availability Statement:

All relevant data are shown in the paper as tables and figure.

Author Contributions

T. Kobari, DH and NY conceived and designed the oceanographic observations and experiments. DH, HN, AN, ET, TM, TN performed the oceanographic observations and turbulence measurements. T. Kobari, TH, T. Kanayama and FK performed the onboard experiments. T. Kobari, TH, T. Kanayama, FK, NY, KS analyzed the samples and data of the onboard experiments. DH and TT analyzed the data of oceanographic observations and turbulence measurements. T. Kobari, GK, HN and XG organized the research cruises.

Competing interests:

The authors declare no competing and conflict interests.

Acknowledgements

We thank the captains and crew of the T/S *Kagoshima Maru* for their help in oceanographic observations and sample collections.

Financial support:

This study has been supported by grants from the Japan Society for the Promotion of Science (17K00522, 18H04920, 4702), Ministry of Education, Culture, Sports, Science and Technology in Japan (The Study of Kuroshio Ecosystem Dynamics for Sustainable Fisheries).

323 **References**

324 Bower, J.R., Nakamura, Y., Mori, K., Yamamoto, J., Isoda, Y., Sakurai, Y.: Distribution of *Todarodes pacificus*

325 (Cephalopoda: Ommastrephidae) paralarvae near the Kuroshio off southern Kyushu, Japan, Mar. Biol., 135,

326 99–106, 1999.

327 Calbet, A., Landry, M. R.: Mesozooplankton influences on the microbial food web: Direct and indirect trophic interactions

328 in the oligotrophic open-ocean, Limnol. Oceanogr., 44, 1370–1380, 1999.

329 Calbet, A., Landry, M. R.: Nunnery S. Bacteria-flagellate interactions in the microbial food web of the oligotrophic

330 subtropical North Pacific, Aquat. Microb. Ecol., 23, 283–292, 2001.

331 Calbet, A., Landry, M. R.: Phytoplankton growth, microzooplankton grazing, and carbon cycling in marine systems.

332 Limnol. Oceanogr., 49, 51–57, 2004.

333 Calbet, A., Saiz, E.: The ciliate-copepod link in marine ecosystems, Aquat. Microb. Ecol., 38, 157–167, 2005.

334 Chen, C. C., Shiah, F.K., Gong, G. C., Chiang, K. P.: Planktonic community respiration in the East China Sea: importance

335 of microbial consumption of organic carbon. Deep-Sea Res. II, 50, 1311–1325, 2003.

336 Cyr, F., Bourgault, D., Galbraith, P. S.: Gosselin M. Turbulent nitrate fluxes in the Lower St. Lawrence Estuary, Canada.

337 J. Geophys. Res., 120, 2308–2330, 2015.

338 Du, C., Liu, Z., Kao, S-J., Dai, M.: Diapycnal fluxes of nutrients in an oligotrophic oceanic regime: the South China Sea.

339 Geophys. Res. Lett., 44, 11510-11518, 2017.

340 Endo, H., Suzuki, K.: Spatial variations in community structure of haptophytes across the Kuroshio front in the Tokara

341 Strait, in: Kuroshio Current, Physical, Biogeochemical and Ecosystem Dynamics, edited by: Nagai, T., Saito, H.,

342 Suzuki, K., Takahashi, M., Geophysical Monograph 243, John Wiley & Sons, Hoboken, 207–221, 2019.

343 Gaines, G., Elbrächter. M.: Heterotrophic nutrition, in The biology of dinoflagellates, edited by: Taylor, F. J. R., Blackwell,
344 Oxford, 224–268, 1987.
345 Guo, Y. J.: The Kuroshio, Part II. Primary production and phytoplankton, Oceanogr. Mar. Bio. Ann. Rev., 29, 155–189,
346 1991.
347 Hansen, B., Bjørnsen, P. K., Hansen, P. J.: The size ratio between planktonic predators and their prey, Limnol.
348 Oceanogr., 39, 395–403, 1994.
349 Hasegawa, D., Island Mass Effect, in: Kuroshio Current, Physical, Biogeochemical and Ecosystem Dynamics, edited
350 by: Nagai, T., Saito, H., Suzuki, K., Takahashi, M., Geophysical Monograph 243, John Wiley & Sons,
351 Hoboken, 163–174, 2019.
352 Hasegawa, D., Tanaka, T., Matsuno, T., Senjyu, T., Tsutsumi, E., Nakamura, H., Nishina, A., Kobari, T., Yoshie, N.,
353 Guo, X., Nagai, T., Okunishi, T., Yasuda, I.: Measuring the vertical turbulent nitrate flux using sensors, Bull.
354 Coast. Oceanogr., 57, 59–64, 2019.
355 Hasegawa, D., Yamazaki, H., Ishimaru, T., Nagashima, H., Koike, Y.: Apparent phytoplankton bloom due to island mass
356 effect, J. Mar. Syst., 69, 238–246, 2008.
357 Hasegawa, D., Yamazaki, H., Lueck, R. G., Seuront, L.: How islands stir and fertilize the upper ocean, Geophys. Res.
358 Lett., 31, L16303, 2004.
359 Hasegawa, T., Kitajima S., Kiyomoto Y.: Phytoplankton distribution in the Kuroshio region of the southern East China
360 Sea in early spring, in: Kuroshio Current, Physical, Biogeochemical and Ecosystem Dynamics, edited by: Nagai,
361 T., Saito, H., Suzuki, K., Takahashi, M., Geophysical Monograph 243, John Wiley & Sons, Hoboken, 191–205,
362 2019.

363 Hirota, Y.: The Kuroshio, Part III. Zooplankton, Oceanogr Mar. Bio. Ann. Rev., 33, 151–220, 1995.

364 Hu, D., Wu, L., Cai, W., Gupta, A. S., Ganachaud, A., Qiu, B., Gordon, A. L., Lin, X., Chen, Z., Hu, S., Wang, G.,

365 Wang, Q., Sprintall, J., Qu, T., Kashino, Y., Wang, F., William S. Kessler, W. S.: Pacific western boundary

366 currents and their roles in climate, Nature, 522, 299–308, 2015.

367 Kaneko, H., Yasuda, I., Komatsu, K., Itoh, S.: Observations of the structure of turbulent mixing across the Kuroshio,

368 Geophys. Res. Lett., 39, L15602, 2012.

369 Kaneko, H., Yasuda, I., Komatsu, K., Itoh, S.: Observations of vertical turbulent nitrate flux across the Kuroshio, Geophys.

370 Res. Lett., 40, 3123–3127, 2013.

371 Kobari, T., Kobari, Y., Miyamoto, H., Okazaki, Y., Kume, G., Kondo, R., Habano, A.: Variability in taxonomic

372 composition, standing stock and productivity of the plankton community in the Kuroshio and its neighboring

373 waters, in: Kuroshio Current, Physical, Biogeochemical and Ecosystem Dynamics, edited by: Nagai, T., Saito,

374 H., Suzuki, K., Takahashi, M., Geophysical Monograph 243, John Wiley & Sons, Hoboken, 223–243, 2019.

375 Kobari, T., Makihara, W., Kawafuchi, T., Sato, K., Kume, G.: Geographic variability in taxonomic composition, standing

376 stock, and productivity of the mesozooplankton community around the Kuroshio Current in the East China Sea,

377 Fish. Oceanogr., 27, 336–350, 2018.

378 Kobari, T., Mitsui, K., Ota, T., Ichinomiya, M., Gomi, Y.: Response of heterotrophic bacteria to the spring phytoplankton

379 bloom in the Oyashio region. Deep-Sea Res. II., 57, 1671–1678, 2010.

380 Komatsu, K., Hiroe, Y.: Structure and impact of the Kuroshio nutrient stream, in: Kuroshio Current, Physical,

381 Biogeochemical and Ecosystem Dynamics, edited by: Nagai, T., Saito, H., Suzuki, K., Takahashi, M.,

382 Geophysical Monograph 243, John Wiley & Sons, Hoboken, 85–104, 2019.

383 Kuroda, H.: The Kuroshio-induced nutrient supply in the shelf and sloe region off the southern coast of Japan, in: Kuroshio
384 Current, Physical, Biogeochemical and Ecosystem Dynamics, edited by: Nagai, T., Saito, H., Suzuki, K.,
385 Takahashi, M., Geophysical Monograph 243, John Wiley & Sons, Hoboken, 137–146, 2019.
386 Landry, M. R., Hasset, R. P.: Estimating the grazing impact of marine micro-zooplankton, Mar. Biol., 67, 283–288,
387 1982.
388 Landry, M. R., Kirshtein, J., Constantinou, J.: A refined dilution technique for measuring the community grazing impact
389 of microzooplankton with experimental tests in the central equatorial Pacific, Mar. Ecol. Prog. Ser., 120, 53–63,
390 1995.
391 Nagai, T., Clayton, S.: Nutrient interleaving below the mixed layer of the Kuroshio Extension front. Ocean Dyn., 67,
392 1027–1046, 2017.
393 Nagai, T., Clayton, S., Uchiyama, Y.: Multiscale routes to supply nutrients through the Kuroshio nutrient stream, in:
394 Kuroshio Current, Physical, Biogeochemical and Ecosystem Dynamics, edited by: Nagai, T., Saito, H., Suzuki,
395 K., Takahashi, M., Geophysical Monograph 243, John Wiley & Sons, Hoboken, 105–125, 2019.
396 Nagai, T., Durán, G. S., Otero, D. A., Mori, Y., Yoshie, N., Ohgi, K., Hasegawa, D., Nishina, A., Kobari, T.: How the
397 Kuroshio Current delivers nutrients to sunlit layers on the continental shelves with aid of near-internal waves
398 and turbulence, Geophys. Res. Lett., 46, 10.1029/2019GL082680, 2019.
399 Nagai, T., Hasegawa, D., Tanaka, T., Nakamura, H., Tsutsumi, E., Inoue, R., Yamashiro, T.: First evidence of coherent
400 bands of strong turbulent layers associated with high-wavenumber internal-wave shear in the upstream Kuroshio,
401 Sci. Rep., 7, 14555, 2017.
402 Nakamura, H., Yamashiro, T., Nishina, A., Ichikawa, H.: Time frequency variability of Kuroshio meanders in Tokara

403 Strait, Geophys. Res. Lett., 33, L21605, 2006.

404 Nakata, K., Hidaka, K.: Decadal-scale variability in the Kuroshio marine ecosystem in winter, Fish. Oceanogr., 12, 234–

405 244, 2003.

406 Nakata, K., Zenitani, H., Inagake, D.: Differences in food availability for Japanese sardine larvae between the frontal

407 region and the waters on the offshore side of Kuroshio, Fish. Oceanogr., 4, 68–79, 1995.

408 Osborn, T.: Estimates of the local rate of vertical diffusion from dissipation measurements. J. Phys. Oceanogr., 10, 83–

409 89, 1980.

410 Parsons, T. R., Takahashi, M., Hargrave, B.: Biological oceanographic processes, Pergamon Press, Oxford, 1984.

411 Pierce, R. W., Turner, J. T.: Ecology of planktonic ciliates in marine food webs, Rev. Aquat. Sci., 6, 139–181, 1992.

412 Putt, M., Stoecker, D. K.: An experimentally determined carbon:volume ration for marine "oligotrichous" ciliates from

413 estuarine and coastal waters, Limnol. Oceanogr., 34, 1097–1103, 1989.

414 Qiu, B.: Kuroshio and Oyashio Currents, in: Encyclopedia of Ocean Sciences, edited by: Steele, J. H., Academic Press,

415 New York, 358–369, 2001.

416 Saito, H.: The Kuroshio: its recognition, scientific activities and emerging issues, in: Kuroshio Current, Physical,

417 Biogeochemical and Ecosystem Dynamics, edited by: Nagai, T., Saito, H., Suzuki, K., Takahashi, M.,

418 Geophysical Monograph 243, John Wiley & Sons, Hoboken, 1–11, 2019.

419 Sassa, C., Tsukamoto, Y.: Distribution and growth of *Scomber japonicus* and *S. australasicus* larvae in the southern East

420 China Sea in response to oceanographic conditions, Mar. Ecol. Prog. Ser., 419, 185–199, 2010.

421 Sassa, C., Tsukamoto, Y., Nishiuchi, K., Konishi, Y.: Spawning ground and larval transport processes of jack mackerel

422 *Tranchurus japonicas* in the shelf-break region of the southern East China Sea, Cont. Shelf. Res., 28, 2574–

423 2583, 2008.

424 Tsutsumi, E., Matsuno, T., Lien, R. C., Nakamura, H., Senjyu, T., Guo, X.: Turbulent mixing within the Kuroshio in the

425 Tokara Strait, J. Geophys. Res. Oceans, 122, 10.1002/2017JC013049, 2017.

426 Uye, S. I., Kasahara, S.: Grazing of various developmental stages of *Pseudodiaptomus marinus* (Copepoda: Calanoida)

427 on naturally occurring particles, Bull. Plankton Soc. Japan, 30, 147–158, 1983.

428 Verity, P. G., Langdon, C.: Relationships between lorica volume, carbon, nitrogen and ATP content of tintinnids in

429 Narragansett Bay, J. Plankton Res., 6, 859–868, 1984.

430 Watanabe, Y., Zenitani, H., Kimura, R.: Offshore expansion of spawning of the Japanese sardine, *Sardinops*

431 *melanostictus*, and its implication for egg and larval survival, Can. J. Fish. Aquat. Sci., 53, 55–61, 1996.

432 Zhu, X. H., Nakamura, H., Dong, M., Nishina, A., Yamashiro, T.: Tidal currents and Kuroshio transport variations in the

433 Tokara Strait estimated from ferryboat ADCP data, J. Geophys. Res., 122, 2120–2142, 2017.

434 **Table 1** Information on locations and environmental conditions at the stations conducted the gradient enrichment (EXP_a)
435 and dilution experiments (EXP_b) in the ECS-Kuroshio. Depth: sampling depth (m) of water samples for each experiment.
436 WT: mean water temperature during the experiments (ºC). $NUTs_o$: nutrients concentrations (μmol L^{-1}) at the beginning
437 of each experiment. CHL_o: Chlorophyll *a* concentration (μgCHL L^{-1}) at the beginning of the experiments. MiZ_o: micro-
438 heterotrophs standing stocks at the beginning of each experiment (μgC L^{-1}). DL: below the detection limit.
439

Station	Location		Date	Year	Depth	WT	NUTs$_o$		CHL$_o$	MiZ$_o$
	Longitude	Latitude					NO_3+NO_2	PO_4		
EXP$_a$										
C02	30°11'N	129°41.0'E	13 Nov	2016	68	26.1	DL	0.02	0.34	0.19
C03	29°50'N	129°08.4'E	13 Nov	2016	75	26.2	DL	0.01	0.41	0.27
F01	29°53'N	129°22.4'E	14 Nov	2016	81	25.1	0.21	0.04	0.35	0.15
G01	29°51'N	129°57.2'E	14 Nov	2016	91	26.1	0.26	0.07	0.44	0.12
K02	29°34'N	128°26.3'E	12 Nov	2017	50	25.6	0.18	DL	0.31	0.23
K05	30°06'N	130°11.9'E	14 Nov	2017	105	24.8	0.57	0.02	0.52	0.79
K08	30°24'N	131°23.6'E	15 Nov	2017	115	25.5	1.82	0.12	0.15	0.34
K11	31°24'N	132°29.2'E	16 Nov	2017	90	25.0	0.16	DL	0.27	0.55
EXP$_b$										
A05a	30°10'N	129°17.5'E	3 Nov	2017	13	25.5	0.10	0.03	0.23	0.12
A05b	30°10'N	129°17.5'E	7 Nov	2017	95	25.5	DL	DL	0.16	0.15
A05c	30°11'N	129°17.2'E	7 Nov	2017	34	25.3	0.02	0.01	0.24	0.05
A06a	30°00'N	129°15.1'E	3 Nov	2017	12	25.4	DL	0.02	0.16	0.13
A06b	30°00'N	129°15.0'E	7 Nov	2017	110	25.7	1.61	0.11	0.14	0.04
A08a	29°19'N	129°09.4'E	6 Nov	2017	76	25.6	DL	0.02	0.29	0.22
A08b	29°26'N	129°12.4'E	6 Nov	2017	71	25.6	0.03	0.01	0.21	0.17
A09a	29°09'N	129°00.0'E	6 Nov	2017	105	25.6	0.11	0.02	0.20	0.15

Table 2 Phytoplankton growth rate (d^{-1}) derived from the gradient enrichment experiments (EXP_a) in the ECS-Kuroshio. Enriched nitrate concentrations (μmol L^{-1}) are shown at the top of each column. A and B: duplicate bottles. Pico: chlorophyll smaller than 2 μm. Nano: chlorophyll between 2 and 11 μm. Micro: chlorophyll larger than 11 μm.

Station	0		0.05		0.15		0.5		0.75		1.5		5	
	A	B	A	B	A	B	A	B	A	B	A	B	A	B
Micro														
C02	-0.108	-0.116	-0.089	-0.082	0.019	-0.073	0.470	0.426	0.422	0.441	0.686	0.798	0.796	0.556
C03	-0.116	-0.118	-0.073	-0.078	-0.004	-0.008	0.453	0.426	0.588	0.706	0.780	0.892	0.862	0.906
F01	0.150	0.159	0.332	0.277	0.282	0.344	0.445	0.495	0.511	0.497	0.490	0.385	0.372	0.467
G01	0.062	0.051	0.135	0.089	0.163	0.108	0.438	0.477	0.795	0.736	0.828	0.969	0.861	0.781
K02	-0.305	-0.282	-0.205	-0.265	-0.113	-0.305	0.264	0.295	0.119	0.097	0.422	0.652	0.831	0.669
K05	-0.147	0.027	0.007	-0.053	0.037	0.084	0.329	0.176	0.263	0.168	0.645	0.716	0.792	0.701
K08	0.348	0.266	0.350	0.315	0.333	0.407	0.361	0.185	0.448	0.416	0.377	0.468	0.403	0.417
K11	-0.062	-0.036	-0.105	-0.092	0.043	-0.081	0.193	0.179	0.514	0.390	0.765	0.730	0.469	0.558
Nano														
C02	-0.479	-0.260	-0.208	-0.409	-0.297	-0.345	-0.050	0.144	0.173	0.151	0.249	0.333	0.330	0.264
C03	-0.275	-0.261	-0.211	-0.257	-0.080	-0.206	0.113	0.031	0.247	0.192	0.363	0.355	0.288	0.256
F01	-0.244	-0.154	-0.286	-0.092	-0.025	0.101	0.182	0.050	0.148	0.039	0.015	0.056	0.104	0.105
G01	-0.304	-0.172	-0.313	-0.189	-0.165	-0.117	-0.063	-0.178	0.100	0.001	0.286	0.325	0.369	0.053
K02	-0.321	-0.149	-0.384	-0.152	0.022	0.035	0.223	0.251	-0.027	-0.135	0.433	0.229	0.559	0.523
K05	-0.389	-0.318	-0.680	-0.546	-0.267	-0.394	-0.484	-0.248	-0.407	-0.458	0.053	-0.034	0.102	0.196
K08	0.353	0.244	0.508	0.472	0.455	0.436	0.406	0.397	0.473	0.369	0.408	0.546	0.380	0.384
K11	-0.138	-0.088	-0.257	-0.243	-0.134	-0.293	0.073	0.026	0.175	0.201	0.296	0.312	0.434	0.501
Pico														
C02	-0.383	-0.188	-0.186	-0.199	-0.119	-0.162	0.188	0.143	0.162	0.241	0.257	0.291	0.377	0.205
C03	-0.202	-0.258	-0.259	-0.282	-0.143	-0.160	0.017	-0.019	0.148	0.191	0.194	0.248	0.230	0.300
F01	-0.071	-0.091	-0.054	-0.032	0.050	0.129	0.205	0.144	0.216	0.141	0.170	0.134	0.031	0.172
G01	0.019	-0.061	0.051	-0.032	0.019	0.008	0.156	0.162	0.323	0.188	0.338	0.308	0.344	0.366
K02	-0.245	-0.253	-0.257	-0.275	-0.243	-0.230	-0.046	0.010	-0.067	-0.101	0.065	-0.030	0.203	0.089
K05	-0.087	0.031	0.014	-0.027	0.103	0.157	0.057	0.261	0.130	0.339	0.316	0.255	0.368	0.404
K08	0.032	0.055	-0.013	0.228	0.262	0.201	0.240	0.069	0.262	0.281	0.177	0.284	0.222	0.327
K11	-0.197	-0.216	-0.194	-0.146	-0.046	-0.071	-0.005	0.033	0.163	0.076	0.236	0.049	0.092	0.179

Table 3 Parameters derived from the dilution experiments (EXP_b) in the ECS-Kuroshio. g_{max}: maximum growth rate (d^{-1}). m: mortality rate by microzooplankton grazing (d^{-1}). g_o: net growth rate measured in the non-enriched and non-diluted bottles (d^{-1}). g_{en}: net growth rate measured in the enriched and non-diluted bottles (d^{-1}). r^2: coefficient of determination defined from the linear regression of the apparent growth rate of total chlorophyll *a* concentrations against dilution factors. p: p-value. Pico: chlorophyll smaller than 2 µm. Nano: chlorophyll between 2 and 11 µm. Micro: chlorophyll larger than 11 µm. Total: total chlorophyll from pico- to micro.

Station	Pico				Nano				Micro				Total					
	g_{max}	m	g_o	g_{en}	g_{max}	m	g_o	g_{en}	g_{max}	m	g_o	g_{en}	g_{max}	m	g_o	g_{en}	r^2	p
A05a	0.283	0.887	0.415	0.681	1.181	1.345	-0.267	0.181	0.913	0.962	0.059	0.045	1.059	0.619	0.199	0.492	0.757	<0.01
A05b	0.931	1.106	-0.109	0.279	1.354	1.050	-0.505	-0.239	0.477	0.583	-0.030	0.107	1.073	1.051	-0.232	0.113	0.901	<0.01
A05c	0.501	0.647	-0.025	0.190	1.298	1.192	-0.183	-0.066	0.313	0.500	-0.269	0.201	0.828	0.752	-0.074	0.122	0.875	<0.01
A06a	0.179	0.814	0.440	0.646	0.865	1.270	0.247	0.341	0.232	0.597	-0.315	0.339	0.941	0.381	0.347	0.550	0.541	<0.01
A06b	0.648	-0.398	-0.869	-1.020	0.947	0.247	-0.789	-0.629	-0.118	-0.037	-0.038	0.065	-0.052	0.711	-0.735	-0.714	0.750	<0.01
A08a	0.434	0.458	-0.097	0.035	1.448	1.289	-0.072	-0.150	0.401	0.564	-0.537	0.181	0.765	0.775	-0.113	0.009	0.856	<0.01
A08b	0.370	0.846	-0.040	0.509	0.652	1.068	-0.259	0.430	0.553	1.122	-0.620	0.529	0.937	0.471	-0.123	0.488	0.693	<0.01
A09a	0.488	0.417	-0.399	-0.026	0.894	0.734	-0.182	-0.082	0.353	0.022	-0.474	-0.235	0.526	0.640	-0.324	-0.052	0.760	<0.01

Table 4 Parameters derived from relationship of phytoplankton growth rates against logarithmically transformed concentrations of enriched nitrate in the gradient enrichment experiments (EXP_a). Slope: sensitivity of phytoplankton growth rate to logarithmically transformed concentrations of enriched nitrate. Intercept: growth potential at the low nitrate concentration. r^2: coefficient of determination defined from the linear regression of growth rate of size-fractionated chlorophyll *a* concentrations against logarithmically transformed concentrations of enriched nitrate. Pico: chlorophyll smaller than 2 μm. Nano: chlorophyll between 2 and 11 μm. Micro: chlorophyll larger than 11 μm.

Station	Pico			Nano			Micro		
	Slope	Intercept	r^2	Slope	Intercept	r^2	Slope	Intercept	r^2
C02	0.281	0.178	0.848	0.370	0.131	0.831	0.458	0.492	0.846
C03	0.295	0.121	0.922	0.308	0.177	0.830	0.560	0.611	0.914
F01	0.074	0.129	0.317	0.120	0.067	0.420	0.077	0.430	0.368
G01	0.203	0.243	0.866	0.272	0.085	0.688	0.448	0.657	0.817
K02	0.213	-0.014	0.883	0.364	0.233	0.726	0.531	0.353	0.872
K05	0.188	0.251	0.772	0.355	-0.165	0.729	0.419	0.439	0.843
K08	0.070	0.231	0.242	-0.038	0.426	0.213	0.045	0.386	0.162
K11	0.167	0.077	0.750	0.394	0.201	0.943	0.403	0.409	0.744

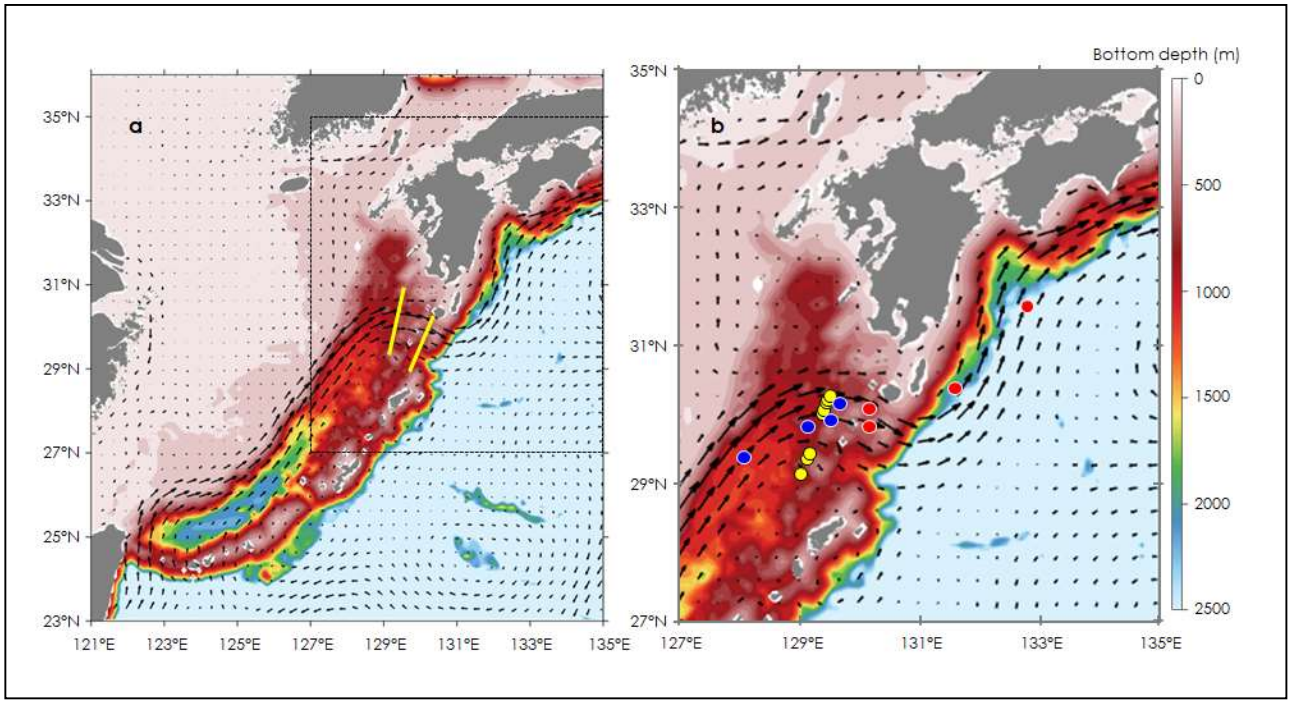

Figure 1 Locations for oceanographic observations and onboard experiments in the Kuroshio Current of the East China Sea (ECS-Kuroshio). **(a)** Oceanographic observations by Deep SUNA V2 and TurboMAP-L (yellow lines). **(b)** Onboard experiments for phytoplankton and microzooplankton growth (EXP_a: red and blue circles) and for microzooplankton grazing (EXP_b: yellow circles). EXP_a are conducted in the upstream (blue circles) and downstream Kuroshio (red circles) in the Tokara Strait. Current directions and velocities (arrows) are shown as monthly means during November 2016. Bottom depth (m) is indicated as colored contours.

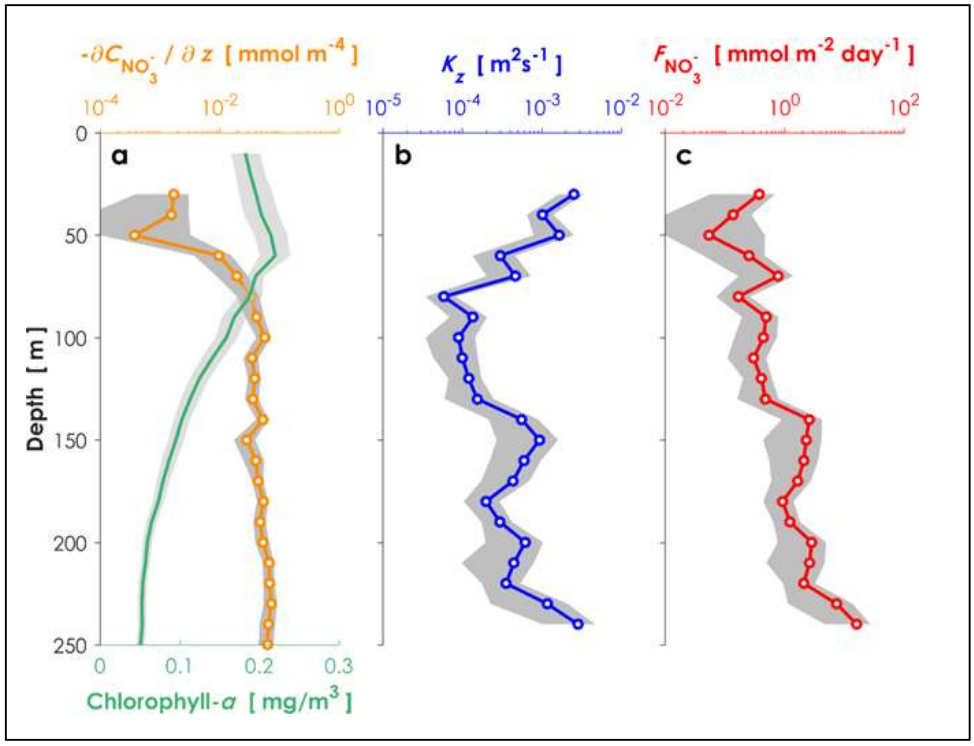

Figure 2 Vertical profiles of environmental conditions in the Kuroshio Current. **(a)** Nitrate gradient curve (orange) and chlorophyll *a* concentrations (green) measured with a nitrate sensor (Deep SUNA V2) attached to an SBE-9plus CTD system. **(b)** Turbulent diffusivity measured with a TurboMAP-L (blue). (**c**) Calculated turbulent nitrate fluxes (red) in the ECS-Kuroshio. The shaded areas are the 95 percent confidence intervals obtained by a bootstrap process.

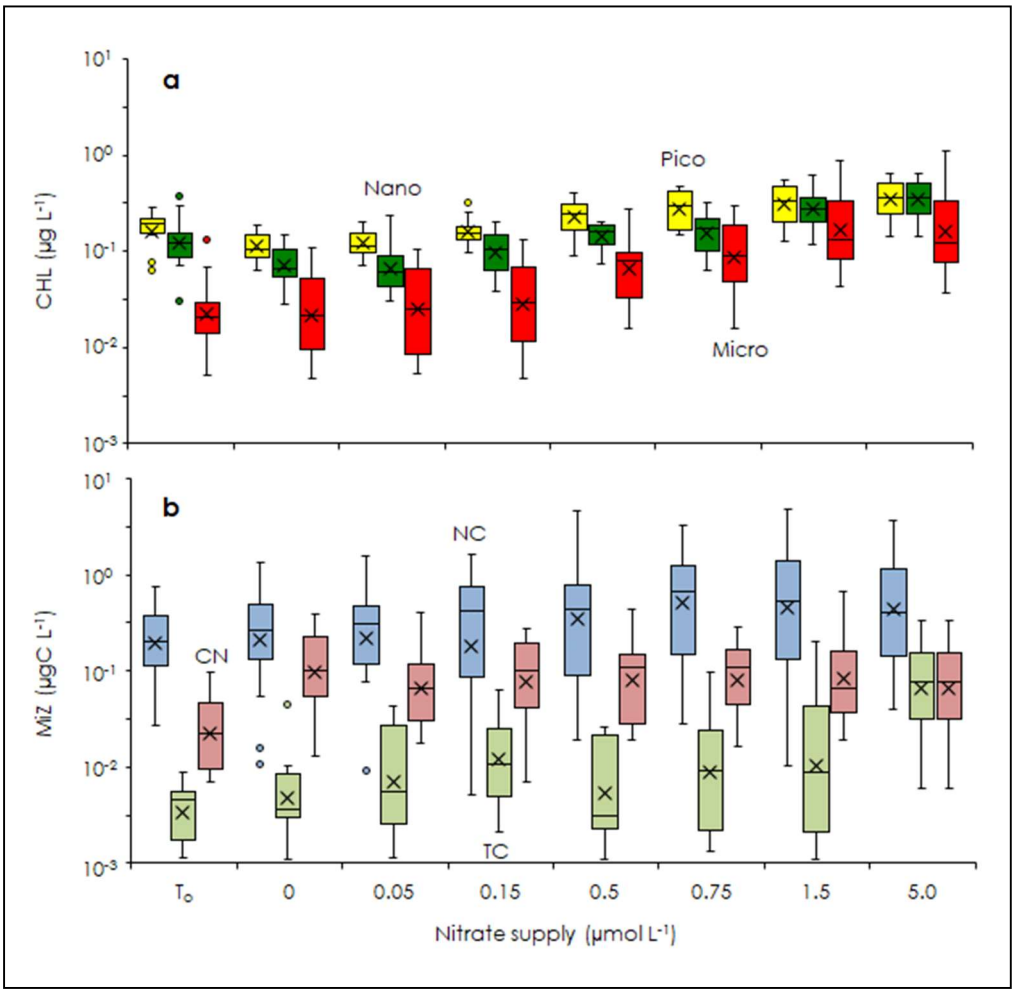

Figure 3 Changes in phytoplankton and micro-sized heterotrophs standing stocks during the gradient enrichment experiments (EXP_a). **(a)** Size-fractionated chlorophyll *a* concentrations (CHL). **(b)** Micro-heterotrophs standing stocks (MiZ). T_o: at the beginning of the gradient enrichment experiments. 0: no enrichment. 0.05 to 5.0 µmol L^{-1}: enrichment. Box-and-whisker diagram at each nitrate concentrations was compiled with the results conducted at the 8 stations. Box represents first (bottom), second (bar) and third (top) quartiles, and cross marks are the average values. Whiskers indicate minimum and maximum values, and circles are outliers. Pico: chlorophyll smaller than 2 µm (yellow). Nano: chlorophyll between 2 and 11 µm (green). Micro: chlorophyll larger than 11 µm (red). NC: naked ciliates (light blue). TC: tintinnid ciliates (light green). CN: copepod nauplii (light pink).

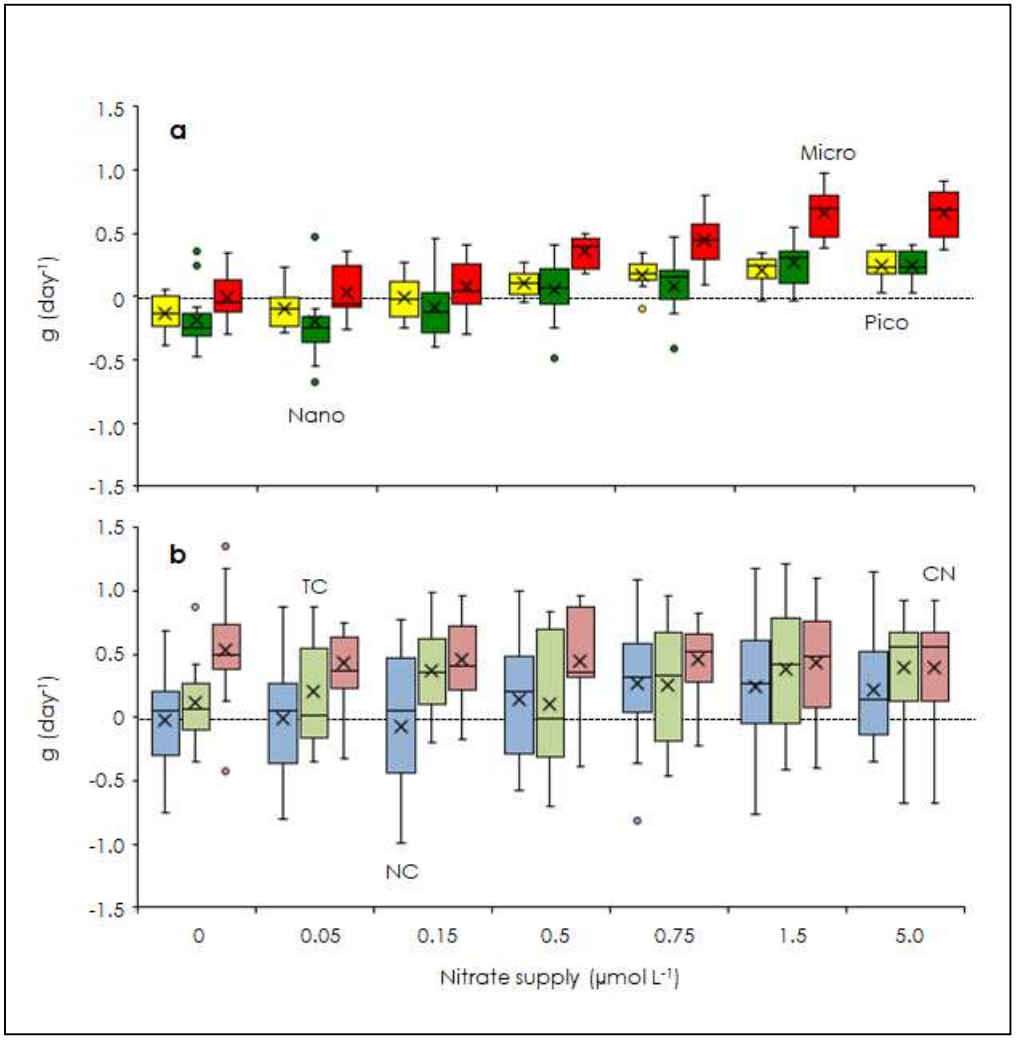

Figure 4 Changes in phytoplankton and micro-sized heterotrophs growth rates in response to nitrate enrichments in the gradient enrichment experiments (EXP_a). **(a)** Growth rates (g: d^{-1}) of size-fractionated chlorophyll. **(b)** Micro-heterotrophs growth rates (g: d^{-1}). 0: no enrichment. 0.05 to 5.0 µmol L^{-1}: enrichment. Box-and-whisker diagram at each nitrate concentration is based on the results conducted at the eight stations. The symbols have the same meaning as in Figure 3.

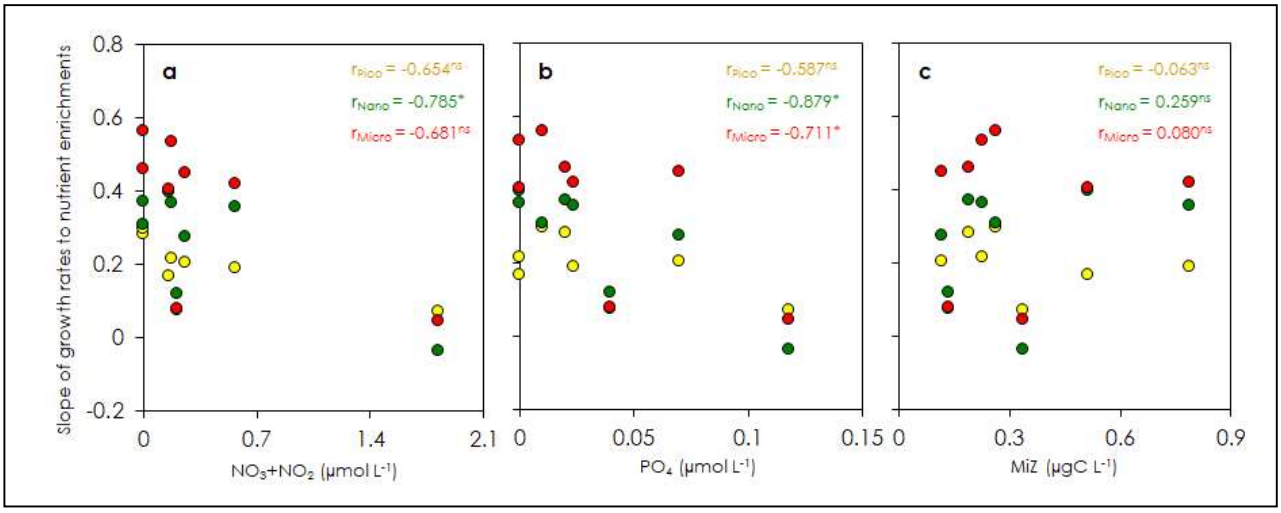

485

486 **Figure 5** Correlation of the regression slopes of phytoplankton growth rates to nutrients concentrations and micro-sized
487 heterotrophs biomass at the beginning of the gradient enrichment experiments (EXP_a). **(a)** Regression slopes of the size-
488 fractionated phytoplankton growth versus the concentrations of nitrate (NO_3) plus nitrite (NO_2). **(b)** Regression slopes of
489 the size-fractionated phytoplankton growth versus the phosphate concentrations (PO_4). **(c)** Regression slopes of the size-
490 fractionated phytoplankton growth versus the micro-heterotrophs biomass (MiZ). r: Pearson correlation coefficient. Pico:
491 chlorophyll smaller than 2 µm. Nano: chlorophyll between 2 and 11 µm. Micro: chlorophyll larger than 11 µm. *: $p<0.05$.
492 ns: no significant.

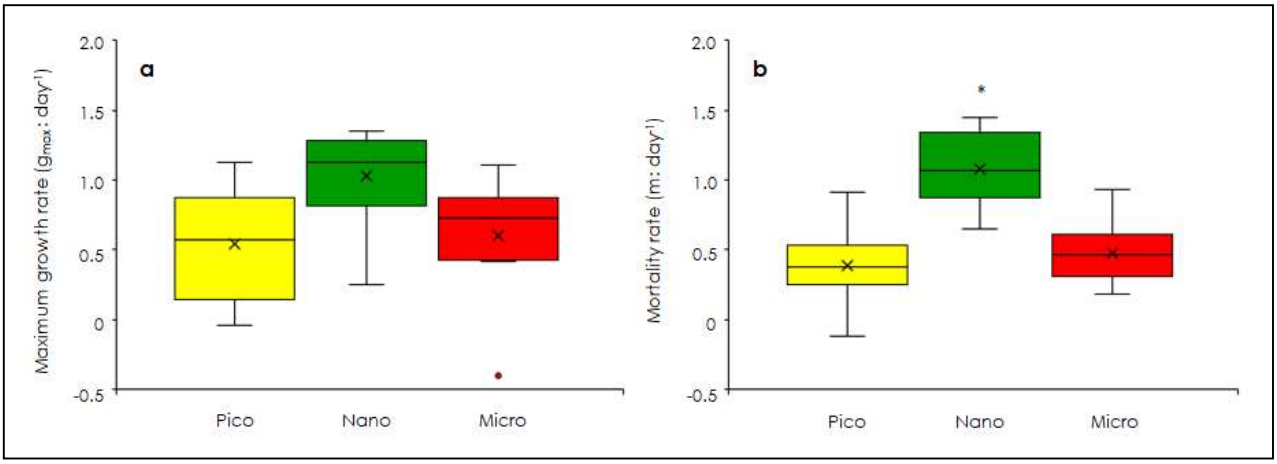

493

494 **Figure 6** Comparisons of phytoplankton growth and mortality rates among the three size-fractionated chlorophyll derived
495 from the dilution experiments (EXP_b). **(a)** Maximum growth rates (g_{max}). **(b)** Mortality rates by mirozooplankton grazing.
496 Box-and-whisker diagram at each nitrate concentrations was compiled with the results conducted at the 8 stations. Box
497 represents first (bottom), second (bar) and third (top) quartiles, and cross marks are the average values. Whiskers indicate
498 minimum and maximum values, and circles are outliers. Asterisk means significant difference among the three size-
499 fractions (ANOVA+Tukey, $p<0.05$). Pico: chlorophyll smaller than 2 μm. Nano: chlorophyll between 2 and 11 μm. Micro:
500 chlorophyll larger than 11 μm.

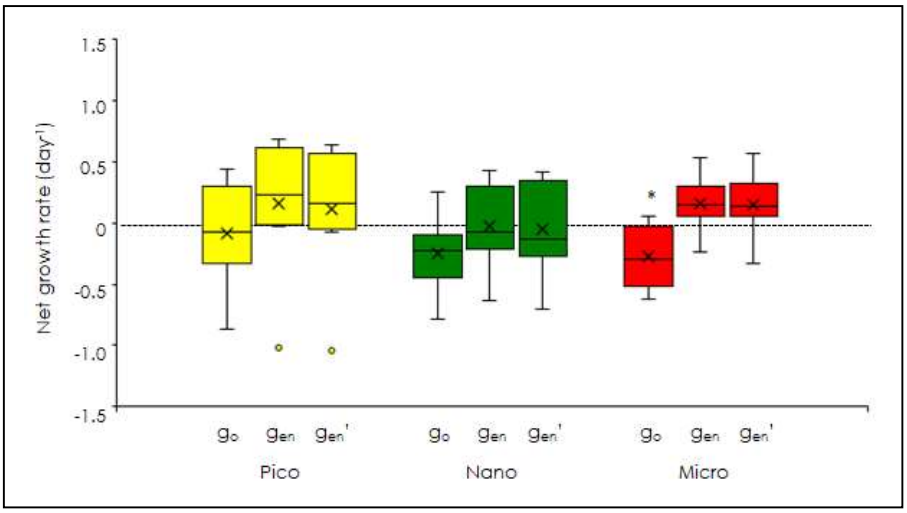

Figure 7 Comparisons of phytoplankton net growth derived from the dilution experiments (EXP_b) among the three different methods. g_o: Observed net growth rates without enrichment in the non-diluted bottles. g_{en}: Observed net growth rates with enrichment in the non-diluted bottles. g_{en}': Estimated net growth rates subtracting the mortality rates (m) from the maximum growth rates (g_{max}). Box-and-whisker diagram at each nitrate concentrations was compiled with the results conducted at the 8 stations. Asterisk means significant difference between g_o and g_{en} (Welch's *t*-test, $p<0.05$). The symbols have the same meaning as in Figure 6.

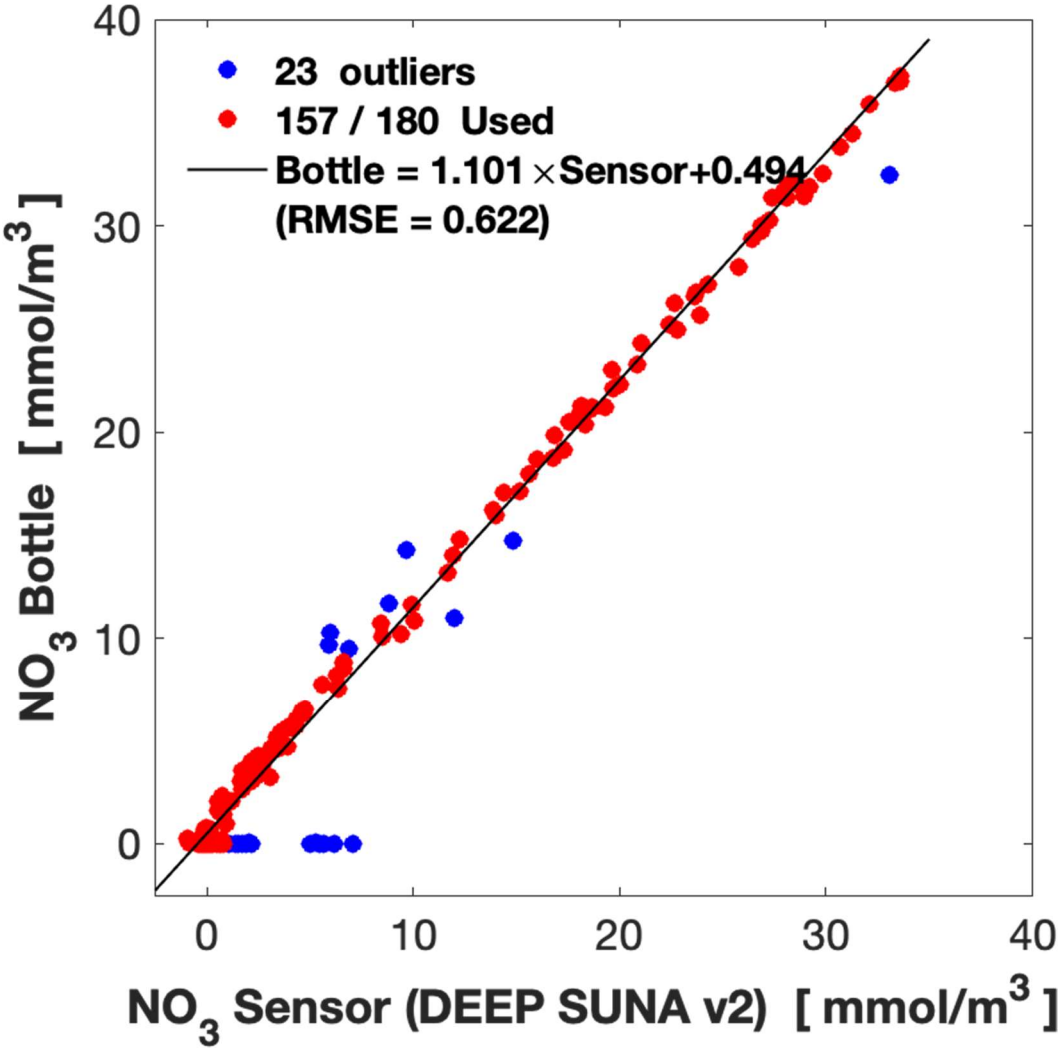

Supplement Figure 1 In situ nitrate measurements by Deep SUNA V2 plotted against the laboratory water analysis results from bottle sampled water in KG1515. For obtaining the regression line used for the sensor calibration, we excluded outlier data in which the absolute value of the difference between the data and regression line exceeded 2.2 times the RMSE.

514

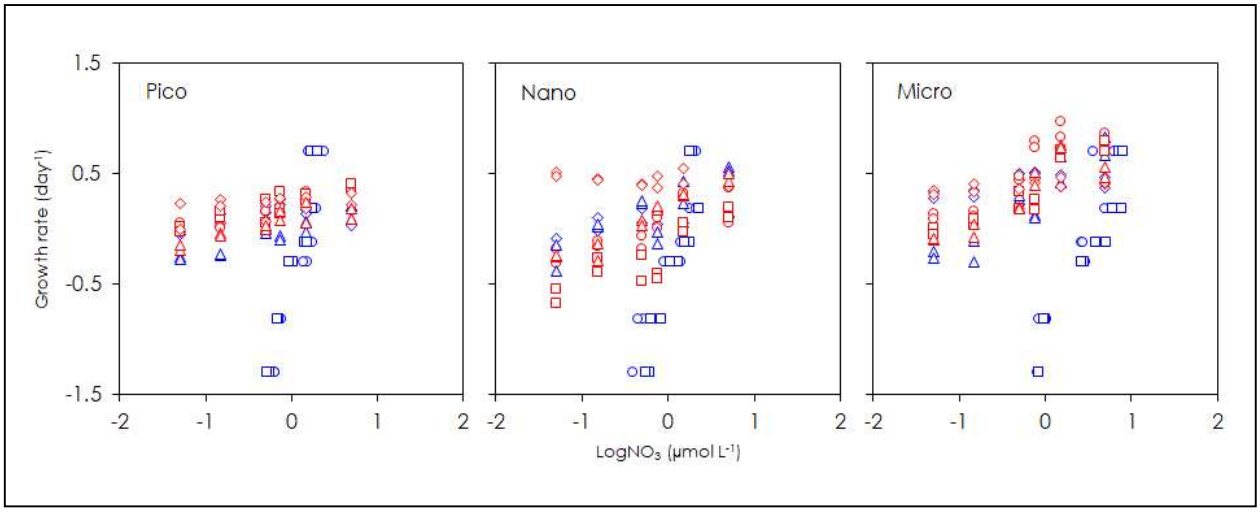

515

516 **Supplement Figure 2** Relationship of phytoplankton growth rates to logarithmically transformed concentrations of
517 enriched nitrate. Blue and red circles mean the stations in the upstream and downstream Kuroshio in the Tokara Strait,
518 respectively. Pico: chlorophyll smaller than 2 μm. Nano: chlorophyll between 2 and 11 μm. Micro: chlorophyll larger
519 than 11 μm.

520